Journal of Aerosol Science 41 (2010) 501–512

Contents lists available at ScienceDirect

Journal of Aerosol Science

journal homepage: www.elsevier.com/locate/jaerosci

Single-scattering properties of tri-axial ellipsoidal mineral dust aerosols: A database for application to radiative transfer calculations

Zhaokai Meng [a], Ping Yang [b,*], George W. Kattawar [a], Lei Bi [a], K.N. Liou [c], Istvan Laszlo [d]

[a] Department of Physics, Texas A&M University, College Station, TX 77843, USA
[b] Department of Atmospheric Sciences, Texas A&M University, College Station, TX 77843, USA
[c] Joint Institute for Regional Earth System Science and Engineering and Department of Atmospheric and Oceanic Sciences, University of California, Los Angeles, CA 90095, USA
[d] NOAA/NESDIS, Center for Satellite Applications and Research, Camp Spring, MD 20746, USA

ARTICLE INFO

Article history:
Received 14 December 2009
Received in revised form
19 February 2010
Accepted 19 February 2010

Keywords:
Dust aerosol
Optical properties
Database

ABSTRACT

This paper presents a user-friendly database software package of the single-scattering properties of individual dust-like aerosol particles for application to radiative transfer calculations in a spectral region from ultraviolet (UV) to far-infrared (far-IR). To expand the degree of morphological freedom of the commonly used spheroidal and spherical models, tri-axial ellipsoids were assumed to be the overall shape of dust-like aerosol particles. A combination of four computational methods, including the Lorenz–Mie theory, the T-matrix method, the discrete dipole approximation, and an improved geometric optics method, was employed to compute the phase matrix, extinction efficiency and single-scattering albedo of ellipsoids with various aspect ratios and sizes. The scattering property database was developed for 42 particle shapes specified in terms of two aspect ratios, 69 refractive indices and 471 size parameters. Additionally, accompanying software, based on interpolation, was developed to provide the single-scattering properties for user-specified aspect ratios, refractive indices and size parameters. The software package allows for the derivation of the bulk optical properties for a given distribution of particle microphysical parameters (i.e., refractive index, size parameter and two aspect ratios). The array-oriented single-scattering property data sets are stored in the NetCDF format.

1. Introduction

Aerosols play an important role in the Earth's climate system through their direct and indirect effects on the energy budget and hydrological cycle of the Earth–atmosphere system (Chylek & Coakley, 1974; Chuang et al., 2003; Forster et al., 2007; Ramanathan, Crutzen, Kiehl, & Rosenfeld (2001); Sokolik et al., 2001; Shell & Somerville, 2007). Mineral dust, an abundant aerosol species primarily originating in desert and semi-arid regions, is distributed over a large area of the globe. The single-scattering properties of mineral dust are fundamental to quantifying aerosol radiative forcing. For this reason, numerous laboratory studies and theoretical modeling simulations have been carried out (e.g. Bi, Yang, Kattawar, & Kahn, 2009, 2010; Clarke et al., 2004; Curtis et al., 2008; Li, Kattawar, & Yang, 2004; Muñoz et al., 2004, 2006; Nousiainen, Kahnert, & Veihelmann, 2006; Sokolik & Toon, 1998; Tegen & Lacis, 1996; Volten et al., 2001, 2006; West, Doose, Eibl, Tomasko, & Mishchenko, 1997; Yang, Kattawar, & Wiscombe, 2004; Yang, et al., 2007; Zubko, Muinonen, Shkuratov, Videen, & Nousiainen, 2007). Measurements of the scattering and polarization properties of sampled dust aerosols have

* Corresponding author.
E-mail address: pyang@tamu.edu (P. Yang).

0021-8502/$ - see front matter © 2010 Elsevier Ltd. All rights reserved.
doi:10.1016/j.jaerosci.2010.02.008

been very valuable in providing the basic data for verification and improvement of the results determined from theoretical calculations and remote sensing techniques. However, due to technical difficulties, experimental determinations of the extinction efficiency, single-scattering albedo and scattering phase matrices around the forward and backward scattering directions have been extremely difficult (Muñoz et al., 2004, 2006; Volten et al., 2001, 2006). Furthermore, measurements are usually conducted at visible wavelengths with a small number of dust samples. The applicability of experimental approaches to the study of the single-scattering properties of dust particles throughout the entire solar and thermal infrared spectra is quite limited. Thus, a comprehensive modeling study, including the selection of particle shape model, simulation of particle optical properties, and comparison between simulation and measurement, is essential to advancing our knowledge and understanding of the optical properties of dust-like aerosols for radiative forcing calculations and remote sensing applications.

Dust particle morphology poses substantial challenges to modeling the optical and microphysical properties (Kokhanovsky, 2003; Nousiainen, 2009). Electron microscope images (e.g., Muñoz & Volten, 2006; Reid, Reid, et al., 2003; Reid, Kinney, & Westphal, 2003) reveal that mineral dust particles are almost exclusively nonspherical and have irregular shapes with no particular habits. A number of researchers (e.g., Feng et al., 2009; Kahn, West, McDonald, Rheingans, & Mishchenko, 1997; Kalashnikova & Sokolik, 2004; Mishchenko, Travis, Rossow, & West, 1997; Mishchenko, Travis, & Lacis, 2003; Yang, Liou, Mishchenko, & Gao, 2000; Yang et al., 2007) have illustrated that modeling of the optical properties of dust particles based on the spherical model, a common shortcut to circumventing modeling challenges, leads to large errors in relevant radiative transfer simulations and remote sensing applications. Nonspherical models, such as the spheroidal model, and relevant computing techniques, were subsequently developed and applied to the analysis of experimental results involving dust particles (e.g., Dubovik et al., 2006; Mishchenko, Travis, Rossow, & West, 1997; Nousiainen, 2009). Based on extensive comparisons between simulated results and experimental data, the spheroidal model, representing a geometrical shape with two degrees of morphological freedom (particle size and aspect ratio) (Dubovik et al., 2006; Schmidt, Wauer, Rother, & Trautmann, 2009), offered a much better solution to the theoretical modeling of the optical properties of dust than its spherical counterpart (Hess, Koepke, & Schult, 1998). Recently, Bi et al. (2009) investigated the single-scattering properties of a tri-axial ellipsoidal model by introducing an additional degree of morphological freedom to reduce the symmetry of spheroids. Their results show the optical properties computed from the ellipsoidal model with optimally selected particle shapes and their weightings closely agree with the laboratory measurements. Furthermore, the results based on the ellipsoidal model fit measurements better than the spheroidal model particularly in the case of the phase matrix elements associated with polarization (Bi et al., 2009).

The objective of this study is to develop a database of the single-scattering properties of tri-axial ellipsoids using a combination of four computational methods including the Lorenz–Mie theory (Bohren & Huffman, 1983), the T-matrix method (Mishchenko et al., 1997; Waterman, 1965), the discrete dipole approximation (DDA) (Purcell & Pennypacker, 1973; Yurkin & Hoekstra, 2009), and an improved geometric optics method (IGOM) (Bi et al., 2009; Yang & Liou, 1996b; Yang et al., 2007). These methods were used to cover various aspect ratios and a size parameter range from Rayleigh to the geometric optics regimes. Specifically, the microphysical properties of the ellipsoidal model were represented in terms of the maximum dimension of the particle, two aspect ratios and the refractive index. To broaden the applicability of this database, the microphysical parameters of particle models have been carefully chosen. The ranges selected for these microphysical properties covered most cases that were employed in previous studies (Dubovik et al., 2006; Levoni, Cervino, Guzzi, & Torricella, 1997). Grid points in the simulation have been selected in a manner to ensure the accuracy of interpolated results for user-defined microphysical parameters. Following Twomey (1977), King, Byrne, Herman, and Reagan (1978), Dubovik and King (2000), and Dubovik et al. (2004, 2006), we have applied the kernel technique to preserve the accuracy in numerical integration for various applications associated with this database.

This paper is organized as follows. Section 2 introduces the dust particle model, morphological parameters and refractive indices. The single-scattering computational methods employed in the development of this database are discussed in Section 3. The database design and user interface are presented in Section 4. In Section 5, typical single-scattering properties selected from the database and their basic features are demonstrated and discussed. A summary of this study is given in Section 6.

2. Dust particle model

A typical tri-axial ellipsoid can be defined in terms of three semi-axis lengths (a, b and c), where a and b are the two semi-minor and semi-major axes of the equatorial ellipse, respectively, and c is the polar radius. For simplicity, the center of the ellipsoid is set at the origin. In principle, the three semi-axis lengths are independent parameters. This database was developed for randomly oriented particles, and it is convenient to assume $c \geq b \geq a$ without loss of generality. Two aspect ratios are defined in terms of $\varepsilon_{a/c}=a/c$ and $\varepsilon_{b/c}=b/c$. Note that $\varepsilon_{a/c}=a/c$ and $\varepsilon_{b/c}=b/c$ are in the range between 0 and 1, which differs from the conventionally defined spheroidal particle aspect ratios that can be larger than unity. As illustrated in Fig. 1, employing the present description of the geometric parameters allows various special geometries (spheres and prolate and oblate spheroids) to be determined by specifying the values of the aspect ratios. The variability of morphology is extended from the cases represented by a range corresponding to $0.3 < \varepsilon_{a/c} < 1$ and $0.3 < \varepsilon_{b/c} < 1$ to the cases denoted by the triangle area indicated by thick lines in Fig. 1. The range of the two aspect ratios of ellipsoid particles is assumed to be

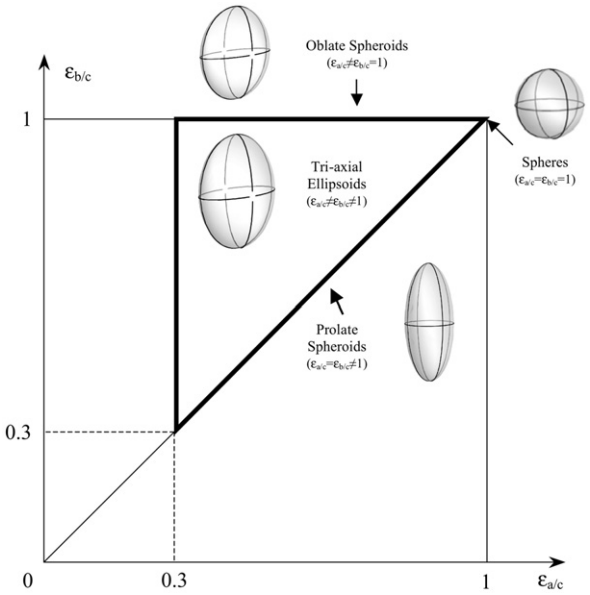

Fig. 1. The morphology of ellipsoids in 2-D aspect-ratio space. The computation domain is the triangle area, including the three sides.

$0.3 \le \varepsilon_{a/c} \le \varepsilon_{b/c} \le 1$, which includes the cases for both spheres and spheroids (Dubovik et al., 2006; Hess, Koepke, & Schult, 1998) as a subset of the present data sets.

Considering that the optical properties of individual dust particles are functions of the size parameter, x, the database was developed in terms of x rather than in the wavelength or size domains. The size parameter was defined with respect to the major axis as $x=2\pi c/\lambda$, where λ is the wavelength of the incident plane wave. In line with previous studies (e.g. Henning, Il'in, Krivova, Michel, & Voshchinnikov, 1999), the range of size parameter was chosen to be $0.025 \le x \le 1000$. The volume-equivalent size parameter can be defined as follows:

$$x_{eff} = x(\varepsilon_{a/c}\varepsilon_{b/c})^{(1/3)} \tag{1}$$

The real and imaginary parts of the complex refractive indices of particle models were set as two independent variables in the database package. In the visible spectral region, the real part of the dust particle refractive index is from 1.5 to 1.6 (Claquin, Schulz, & Balkanski, 1999; Nousiainen, 2009; Sokolik & Toon, 1999), and the imaginary part is set to be 0.0015 or smaller (Haywood et al., 2003; Nousiainen, Muinonen, & Raisanen (2003); Sokolik & Toon, 1999). According to the refractive index data compiled by Levoni et al. (1997), the ranges of the real and imaginary parts of dust refractive indices from 0.2 μm to 40 μm are as follows: $1.10 \le m_r \le 2.10$ and $0.005 \le m_i \le 0.6$. In order to cover all the possibilities for the refractive indices of dust in the visible and infrared spectral regions in this database, we have selected the following: $1.10 \le m_r \le 2.10$ and $0.0005 \le m_i \le 0.5$. For cases with large m_r (≥ 1.7), m_i was assumed to be larger than 0.1, as the absorption of dust particles was usually high (Levoni et al., 1997). Figs. 2a and b show the selected ranges and the data compiled by Levoni et al. (1997) for the real and imaginary parts of the dust complex refractive index. In each panel, the area between the two dashed lines is the selected range and the solid line is the data of Levoni et al. (1997) for feldspar dust particles. Thus, the database is applicable to remote sensing and radiative transfer studies in a spectral region from visible to thermal infrared.

The present database has five dimensions including two aspect ratios, one size parameter, and two parts of the complex refractive indices. Due to the substantial computer time required, the optical properties of dust particles were computed at the selected grid points of the microphysical parameters listed in Tables 1 and 2. Higher resolutions of grid points were chosen in the cases corresponding to the small imaginary part of the refractive index, the small size parameters and the shapes close to spheres. These were chosen because the optical properties are sensitive to variations in the corresponding variables in those parameter regions. The grid points in the size parameter dimension were selected according to a logarithmical scale, as shown in Table 2. Dubovik et al (2006) demonstrated that the single-scattering properties of dust particles showed smoother variations with logarithmically spaced intervals than with uniformly spaced intervals. The optical properties at user-defined grid points in the five-dimensional parameter space can be obtained through the interpolation approach incorporated in the accompanying computer programs.

3. Computational methods

A general tri-axial ellipsoid is a standard quadratic surface in mathematics; however, computing its optical properties over a complete range of size parameters from Rayleigh to the geometric optics domains is a challenging computational

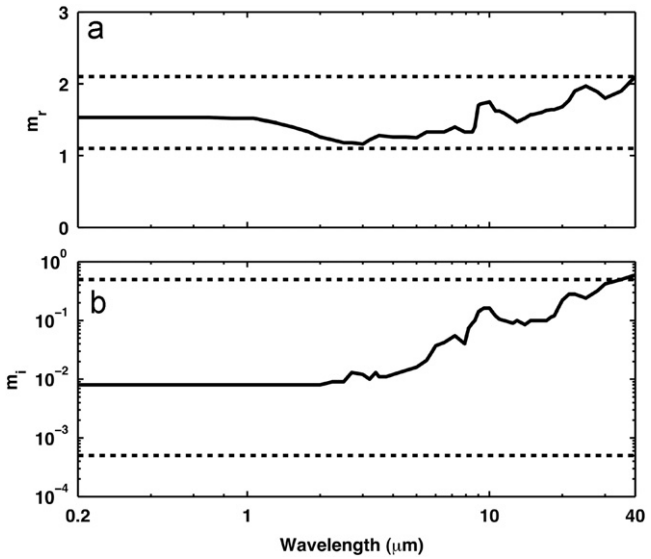

Fig. 2. Complex refractive indices of dust and the simulation domain (the area between two dashed lines). The data was taken from Levoni et al. (1997).

Table 1
The selected aspect ratios and refractive indices for the present scattering simulations.

Microphysical properties	Values
Refractive Index (Real Part)	1.1, 1.2, 1.3, 1.4, 1.5, 1.6, 1.7, 1.9, 2.1
Refractive Index (Imaginary Part)	0.0005, 0.001, 0.005, 0.01, 0.02, 0.05, 0.08, 0.1, 0.2, 0.5
Aspect Ratio ($\varepsilon_{a/c}$ & $\varepsilon_{a/c}/\varepsilon_{b/c}$)	1, 0.98, 0.95, 0.91, 0.88, 0.86, 0.83, 0.67, 0.56, 0.48, 0.42, 0.37, 0.30

Table 2
Size parameter resolutions selected for simulations. Blank cells indicate that simulations were not conducted for the computational method.

Technique	Equidistant sampling interval of size parameter							
	0.025–0.50	0.50–2.50	2.50–10.00	10.00–20.00	20.00–40.00	40.00–100.00	100.00–250.00	250.00–1000.00
ADDA	0.025	0.05	0.50	1	2			
T-matrix	0.025	0.025	0.25	0.25	0.25			
Lorenz–Mie	0.025	0.025	0.025	0.25	0.25	0.25	0.25	0.25
IGOM				1	2	2.5	5	25

endeavor. At present, there are several computational methods that can be applied to ellipsoidal particles. For small particles, three popular methods have usually been employed, the DDA method (Draine & Flatau, 1994; Purcell & Pennypacker, 1973; Yurkin & Hoekstra, 2009), the finite difference time domain (FDTD) method (Sun, Fu, & Chen, 1999; Yee, 1966; Yang & Liou, 1996a), and the T-matrix method (Mishchenko et al. 1997; Waterman, 1965). The DDA and the FDTD methods have comparable efficiency and applicability. The T-matrix method lends itself more easily to spheroids than to tri-axial ellipsoids. At present, no single method can efficiently and accurately determine the optical properties of large ellipsoidal particles. For large nonspherical particles, the only approximate approaches that are available are based on the principles of geometric optics (e.g., Yang & Liou 1996b; Yang et al., 2007).

Bi et al. (2009) investigated the scattering of light by ellipsoids using a combination of the DDA and IGOM methods. The edge effects in the semi-empirical scattering theory (Nussenzveig, 1992) have been incorporated into the efficiency factors in the IGOM. The curvature radius of the profile of the penumbra region (Nussenzveig, 1992) was an essential geometric parameter and should be taken into account in merging the extinction efficiencies and single-scattering albedos simulated from the two methods. Relatively accurate single-scattering properties of tri-axial ellipsoids can be obtained for all size parameters using the DDA and the modified IGOM.

In this study, for tri-axial ellipsoids without rotational symmetry (i.e., $\varepsilon_{a/c} \neq 1$, $\varepsilon_{b/c} \neq 1$, and $\varepsilon_{a/c} \neq \varepsilon_{b/c}$) and for spheroids with extreme aspect ratios, a combination of the DDA and IGOM was employed to calculate their optical properties. The

T-matrix method, combined with the IGOM, was applied to the computation of the single-scattering properties of spheroids with small and moderate aspect ratios, whereas the Lorenz–Mie theory was used in the calculation for the sphere model. Different scattering methods have different applicable regions in terms of the size parameter. The DDA method was applied to determine the single-scattering properties for tri-axial ellipsoids with x_{eff} smaller than 17. The T-matrix method was used for spheroids with x_{eff} smaller than 30. The Lorenz–Mie theory can provide single-scattering properties covering all size parameters associated with the spherical model. The remaining cases were solved by the IGOM. Computer codes for the four aforementioned scattering methods used in the simulations were: Lorentz–Mie code (Bohren & Huffman, 1983); T-matrix code (Mishchenko & Travis, 1998); Amsterdam DDA (commonly known as ADDA) code (Yurkin & Hoekstra, 2009); and IGOM code (Bi et al., 2009; Yang & Liou, 1996b; Yang et al. 2007).

To ensure the accuracy of DDA calculations, the criterion, $dpl=10|m|$, was applied, where dpl stands for 'dipoles per lambda' and represents the dipole density. In order to derive the single-scattering properties for randomly oriented particles, we have calculated $33\times9\times5$ different orientations within the ranges $0^\circ\le\alpha\le360^\circ$, $0^\circ\le\beta\le90^\circ$, and $0^\circ\le\gamma\le90^\circ$, which were based on the symmetric properties of ellipsoids, where α, β and γ are three Euler angles specifying the particle orientations. Results for different orientations were averaged and saved to represent the optical properties for individual randomly oriented ellipsoids. For the T-matrix and IGOM simulations, the computational parameters in the codes were employed without additional modifications.

4. Database design and user interface

The structure of the present database and the logical flow for its application to the determination of the bulk optical properties of dust-like aerosols and the retrieval of dust microphysical properties from remote sensing measurements are illustrated in Fig. 3. The database provides the single-scattering properties of dust particles with pre-defined microphysical and optical parameters, i.e., particle size parameter, aspect ratios and refractive index. The single-scattering properties of an individual dust particle are the extinction efficiency, single-scattering albedo and phase matrix. The notation "Shape 1" refers to the selected shapes used for computation. For each shape, 69 refractive indices were selected for simulation and noted as "Refr. Index". The single-scattering properties for each model were subsequently determined and properly arranged to form the database.

By utilizing the database, the physical properties of dust-like aerosol ensembles, such as size distribution, shape distribution and refractive index can be retrieved from remote sensing measurements by using, for example, a method

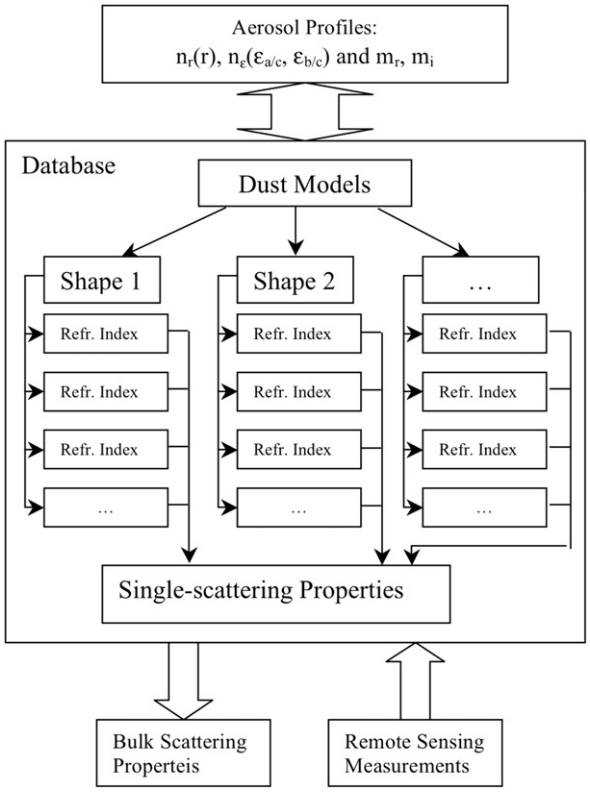

Fig. 3. The basic logic flow of this database.

developed by Dubovik et al. (2006). On the other hand, based on the aerosol microphysical properties including particle size and aspect ratio distributions, the bulk scattering properties of an ensemble of aerosol particles can be derived from the single-scattering properties contained in the database. It should be pointed out that it is quite challenging to accurately simulate backscatter and the present database is more suitable in terms of accuracy for passive remote sensing based on satellite observations than it is for lidar studies.

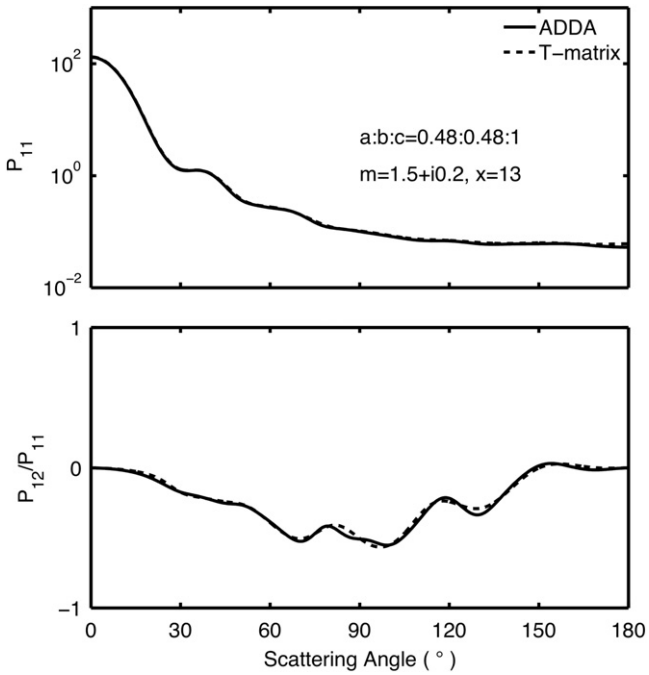

Fig. 4. Comparison of the phase functions and P_{12}/P_{11} computed from the T-matrix and ADDA methods. The size parameter is 13. The ratio of three radii is a:b:c=0.48:0.48:1. The refractive index is 1.5+i0.2.

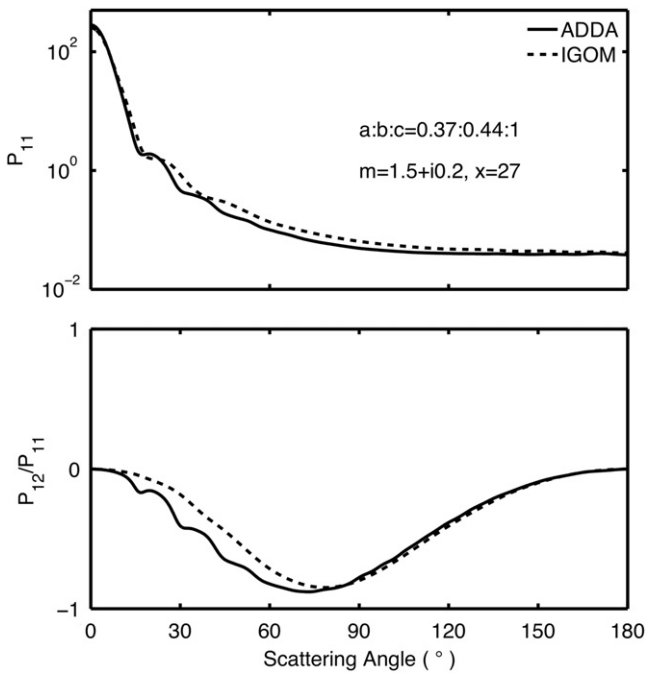

Fig. 5. Comparison of the phase functions and P_{12}/P_{11} computed from the ADDA and the IGOM. The size parameter is 27. The ratio of three radii is a:b:c=0.37:0.44:1. The refractive index is 1.5+i0.2.

In this study, we have applied the kernel technique and formatted the single-scattering properties of particle models in the kernel form. The kernel technique, first introduced by Twomey (1977), has been shown to have a number of advantages in recent studies (e.g. Dubovik et al. 2002, 2006; Levy, Remer, Mattoo, & Vermote, 2007; Nakajima, 1996; Verhaege, Shcherbakov, & Personne, 2009). The technique has both enhanced the accuracy of results and increased the efficiency of retrieval procedures.

The number distribution, $dN_x(x)/d\ln x$, rather than the volume distribution in Dubovik et al. (2006), was applied in building the kernel look-up table of this database. The linear dependence $dN_x(x)/d\ln x = A\ln x + B$ (when $x_l \le x \le x_{l+1}$) was used and coupled with the explicit expression of the kernel function in the form

$$K_{ij}(\ldots;x_l) = \int_{\ln(x_l)}^{\ln(x_{l+1})} \frac{\ln(x_{l+1})-\ln x}{\Delta\ln x} P_{ij}(\ldots;x) c_{sca}(\ldots;x) d\ln x + \int_{\ln(x_{l-1})}^{\ln(x_l)} \frac{\ln x-\ln(x_{l-1})}{\Delta\ln x} P_{ij}(\ldots;x) c_{sca}(\ldots;x) d\ln x \tag{2a}$$

$$K_{sca/ext/abs}(\ldots;x_l) = \int_{\ln(x_l)}^{\ln(x_{l+1})} \frac{\ln(x_{l+1})-\ln x}{\Delta\ln x} c_{sca/ext/abs}(\ldots;x) d\ln x + \int_{\ln(x_{l+1})}^{\ln(x_l)} \frac{\ln x-\ln(x_{l-1})}{\Delta\ln x} c_{sca/ext/abs}(\ldots;x) d\ln x \tag{2b}$$

where x_l $(0 \le l \le 100)$ indicate the lower and upper limits of the size bins. P_{ij} indicates the normalized phase matrix; $c_{sca/ext/abs}$ is the scattering/extinction/absorption cross section and $K\ldots$ indicates the kernels. In this study, 100 size-bins were applied in the database. The centers of the size-bins were logarithmically equidistantly spaced; therefore, the bulk scattering properties averaged in terms of a certain size distribution can be expressed as

$$\overline{c}_{sca}(\ldots)\overline{P}_{ij}(\ldots;\Theta) = \sum_m \frac{dN_x(x^m)}{d\ln x} K_{ij}(\ldots;\Theta;x^m) \tag{3}$$

$$\overline{c}_{sca/ext/abs}(\ldots) = \sum_m \frac{dN_x(x^m)}{d\ln x} K_{sca/ext/abs}(\ldots;x^m) \tag{4}$$

where $\overline{c}_{sca/ext/abs}(\ldots)$ is the averaged scattering, extinction, or absorption cross section of a dust particle ensemble, $\overline{P}_{ij}(\ldots;\Theta)$ are the elements of an averaged phase matrix, and $x^m (1 \le m \le 100)$ is the center of the mth size-bin. The notation "…"in Eqs. (3) and (4) denotes other parameters of the particle ensemble, such as refractive index and aspect ratio.

NetCDF format (http://www.unidata.ucar.edu/software/netcdf) was used to organize the database to make it easily manageable and freely available for major computer languages. The database is split into many small files. Each file stores

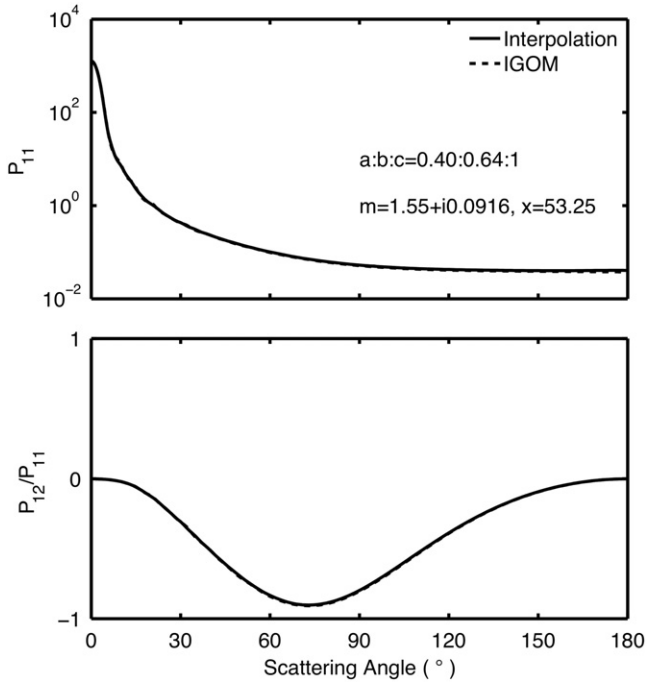

Fig. 6. Comparison between interpolated and simulated results. The size parameter is 53.25. The ratio of three radii is a:b:c=0.40:0.64:1. The refractive index is 1.55+i0.0916.

the optical properties of one ellipsoid class having the same aspect ratio and refractive index. It follows that size parameter is the only variable related to the physical properties of dust within each NetCDF file.

The structure of the individual NetCDF files can be briefly described as follows. In each file, only one variable named "Database" exists. For each variable, there are three dimensions, which are named "x", "pos" and "angle". The first dimension "x" denotes the size parameter, x, which has the sampling points that are logarithmically equidistantly distributed from 0.025 to 1000. The second dimension "angle" represents the scattering angle, which has 500 sampling points listed in the corresponding files in the software package. The last dimension "pos" represents the position of an element in the phase matrix. Additionally, the extinction efficiency, the single-scattering albedo and the asymmetry factor can be found in this database.

All data saved in the database files can be read and written by either the programs contained in the database package, or by a third-party program (in most major computer languages) provided by users. Detailed instructions of how to read and write data from the database files are included in the database document.

5. Results and discussion

Fig. 4 compares the phase functions and P_{12}/P_{11} of randomly oriented spheroids computed from the ADDA and the T-matrix method. Results of the two methods agree quite well. Since the T-matrix method is a rigorous computational technique for randomly oriented spheroidal particles, the agreement between the ADDA and T-matrix methods indicates that the parameters (e.g., the number of particle orientations) chosen for the ADDA calculations are appropriate.

Fig. 5 compares the phase functions and P_{12}/P_{11} computed by the ADDA and IGOM. The solid and dashed lines represent the phase matrix elements computed by the ADDA and IGOM, respectively, which match well except for some slight discrepancies. The ADDA result for P_{12}/P_{11} displays some oscillations whereas the IGOM counterpart is quite smooth. This

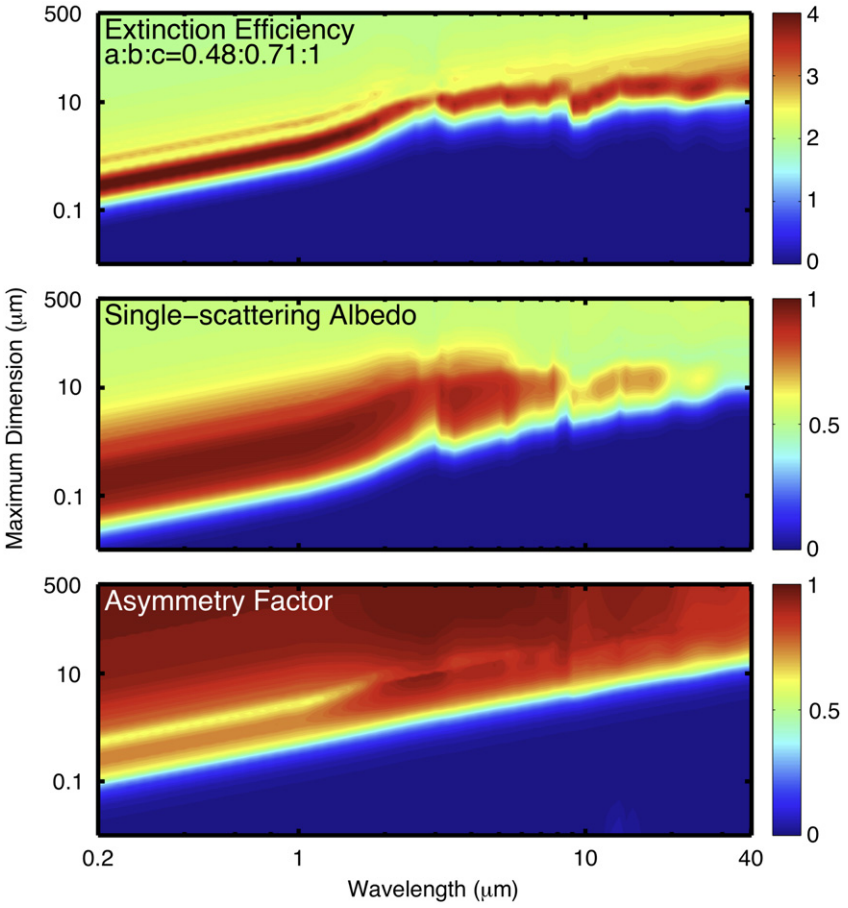

Fig. 7. Contours of the extinction efficiency, single-scattering albedo and asymmetry factor of an ellipsoidal model as functions of wavelength and maximum particle dimension.

is partly due to the limitation of the accuracy of the IGOM and the number of particle orientations considered in the ADDA calculation (Liu, 2008; Penttila et al., 2007).

For ellipsoidal particles whose microphysical parameters do not coincide with the grids, the optical properties can be obtained from an interpolation method. As an example, Fig. 6 shows the comparison between the interpolated results and its counterparts computed directly from the IGOM. In Fig. 6, a relatively strong absorptive case was chosen in which the aspect ratios were set as $\varepsilon_{a/c}$=0.40 and $\varepsilon_{b/c}$=0.64, the refractive index was set to be 1.55+i0.0916, and the size parameter was set at 53.25. None of these microphysical parameters coincide with the grid points chosen for this database; however, the interpolation and computed results matched quite well. The comparison between the interpolated results and those from the direct simulations, demonstrates that the resolution of the grid points is reasonable and interpolation based on these grid points can be considered as accurate.

Fig. 7 shows contours for the extinction efficiency, the single-scattering albedo and the asymmetry factor as functions of wavelength and maximum dimension of an ellipsoidal model with a:b:c=0.48:0.71:1.00. The relationship between wavelength and the complex refractive index of dust is the same as that shown in Fig. 2 (Levoni et al. 1997). The upper left corner of each figure corresponds to large size parameters associated with short wavelengths and large particle sizes, revealing that the values approach the geometric asymptotic limit (2 for the extinction efficiency, 0.53 for the single-scattering albedo, and 1 for the asymmetry factor). The lower right corners of the figures correspond to small size parameters with values approaching zero. The diagonal line (from lower left to upper right) in each panel corresponds to moderately sized particles, mostly found in the resonance region. It is evident from Fig. 7 that the three single-scattering properties vary rapidly along the diagonal lines. For both extinction efficiency and single-scattering albedo, oscillations exist at wavelengths of approximately 3 and 10 μm, because both the real and imaginary parts of the refractive index vary significantly in these spectral regions.

Fig. 8 shows the bulk scattering properties of a mixture of particle shapes, which is obtained by averaging the single-scattering properties over a range of sizes and shapes. The size distribution used is based on the Amsterdam light scattering database (Muñoz et al., 2006), in which the weights of different shapes have been chosen to minimize differences in the phase function between the theoretical results and experimental measurements. The wavelength of the incident beam is set as 0.6328 μm, corresponding to a refractive index of 1.60+i0.01. The dashed lines in Fig. 8 are the results computed from the spherical model according to the size distributions given in the Amsterdam light scattering database. In the theoretical simulation, six sets of aspect ratios, a:b:c=0.48:0.71:1, 0.37:0.56:1, 0.30:0.45:1, 0.37:0.78:1, and 0.30:0.64:1, were assumed, whose weights were 0.0566, 0.2830, 0.0943, 0.2830, 0.1887, and 0.0943. Comparison of the

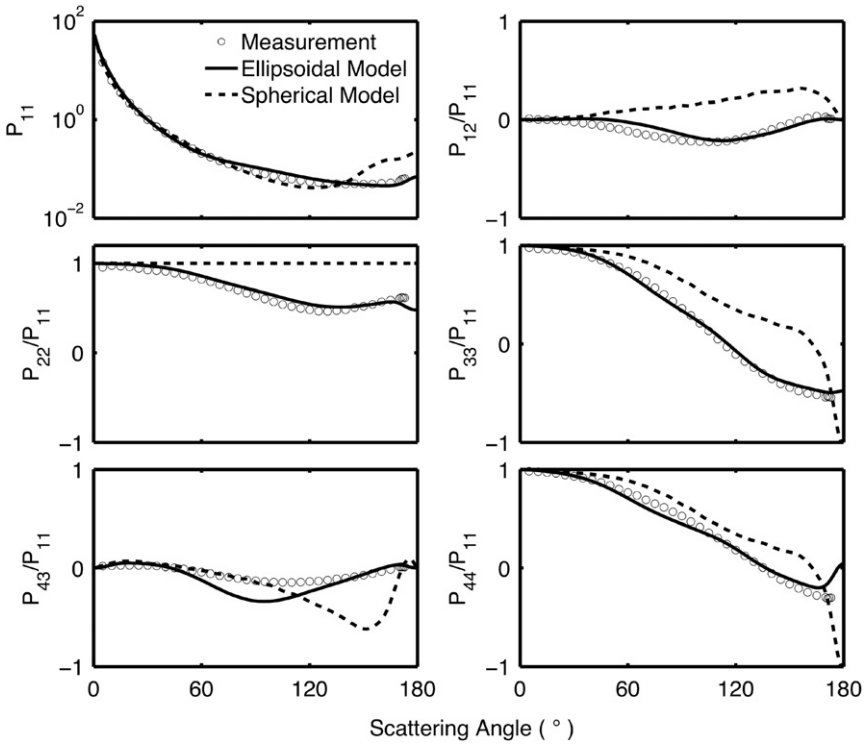

Fig. 8. Comparison between the measured phase matrix (Volten et al. 2006) and the simulated phase matrix for an ensemble of ellipsoids and for sampled Feldspar aerosols at a wavelength of 0.6328 μm. Six sets of aspect ratios are used in this comparison: a:b:c=0.48:0.71:1, 0.37:0.56:1, 0.30:0.45:1, 0.37:0.78:1, 0.30:0.64:1 and 0.30:0.81:1. The weights for the six ellipsoids are 0.0566, 0.2830, 0.0943, 0.2830, 0.1887, and 0.0943.

two models (i.e., the tri-axial ellipsoidal and spherical models) illustrates that the ellipsoidal model provides a better fit to experimental measurements than the spherical model.

6. Summary

The single-scattering properties of dust particles are computed from a combination of the Lorenz–Mie theory, the ADDA method, the T-matrix method, and the IGOM method. The tri-axial ellipsoidal model was used to mimic the overall shapes of dust particles with size parameters ranging from 0.025 to 1000 to ensure applicability of the database to most practical cases. For each size parameter, 42 different shapes and 69 different complex refractive indices were selected for simulations. The selection is applicable to simulating the dust optical properties in visible and infrared spectral regions. Utilizing the kernel technique, the optical properties of the ellipsoidal model have been determined and stored as the kernel look-up table. The data is saved in the database files in NetCDF format to ensure that it is available for all major computer languages. A detailed document for the database and accompanying computer programs to extract the data sets are included in the software package.

The database is suitable for analyzing remote sensing measurements based on observations from satellite and ground-base instruments (Holben et al., 1998; King, Kaufman, Tanré, & Nakajima, 1999; Deuzé et al., 2000; Kaufman, Tanré, & Boucher, 2002; Deuzé et al, 2001). By applying the averaging procedure, the bulk scattering properties can be derived from the database. Comparison between the measured optical properties of dust particles with those computed from the spherical model and a mixture of various ellipsoidal particles demonstrates the advantage of the tri-axial ellipsoidal model.

Acknowledgments

This research is supported by the National Science Foundation under grant ATM-0803779 managed by Dr. Bradley Smull. The authors thank Michael I. Mischenko for the use of his T-matrix code, M. A. Yurkin and A. G. Hoekstra for the use of their ADDA code, and C. F. Bohren and R. Huffman for the use of their Mie code. The database reported in this paper is available upon request.

References

Bi, L., Yang, P., Kattawar, G. W., & Kahn, R. (2009). Single-scattering properties of triaxial ellipsoidal particles for a size parameter range from the Rayleigh to geometric-optics regimes. *Applied Optics*, *48*(1), 114–126.

Bi, L., Yang, P., Kattawar, G. W., & Kahn, R. (2010). Modeling optical properties of mineral aerosol particles by using nonsymmetric hexahedra. *Applied Optics*, *49*(3), 334–342.

Bohren, C. F., & Huffman, D. R. (1983). *Absorption and scattering of light by small particles*. New York: Wiley-Interscience.

Chylek, P., & Coakley, J. (1974). Aerosols and Climate. *Science*, *183*(4120), 75–77.

Claquin, T., Schulz, M., & Balkanski, Y. J. (1999). Modeling the mineralogy of atmospheric dust sources. *Journal of Geophysical Research-Atmospheres*, *104*(D18), 22243–22256.

Clarke, A. D., Shinozuka, Y., Kapustin, V. N., Howell, S., Hubert, B. Doherty, S., et al. (2004). Size distributions and mixtures of dust and black carbon aerosol in Asian outflow: Physiochemistry and optical properties. *Journal of Geophysical Research*, *109*(D15), S09.

Chuang, P. Y., Duvall, R. M., Bae, M. S., Jefferson, A., Schauer, J. J. Yang, H., et al. (2003). Observations of elemental carbon and absorption during ACE-Asia and implications for aerosol radiative properties and climate forcing. *Journal of Geophysical Research*, *108*(D23), 8634.

Curtis, D. B., Meland, B., Aycibin, M., Arnold, N. P., Grassian, V. H. Young, M. A., et al. (2008). A laboratory investigation of light scattering from representative components of mineral dust aerosol at a wavelength of 550 nm. *Journal of Geophysical Research*, *113*(D08210), 1–15.

Draine, B. T., & Flatau, P. J. (1994). Discrete-dipole approximation for scattering calculations. *Journal of the Optical Society of America A*, *11*(4), 1491–1499.

Deuzé, J. L., Bréon, F. M., Devaux, C., Goloub, P., Herman, M. Lafrance, B., et al. (2001). Remote sensing of aerosols over land surfaces from POLDER-ADEOS-1 polarized measurements. *Journal of Geophysical Research*, *106*(D5), 4913–4926.

Deuzé, J. L., Gouloub, P., Herman, M., Marchand, A., Perry, G. Susana, S., et al. (2000). Estimate of the aerosol properties over the ocean with POLDER. *Journal of Geophysical Research*, *105*(D12), 15329–15346.

Dubovik, O. (2004). *Optimization of numerical inversion in photopolarimetric remote sensing, photopolarimetry in remote sensing*. Dordrecht, Netherlands: Kluwer Academic Publishers.

Dubovik, O., & King, M. (2000). A flexible inversion algorithm for retrieval of aerosol optical properties from Sun and sky radiance measurements. *Journal of Geophysical Research-Atmospheres*, *105*(D16), 20673–20696.

Dubovik, O., Holben, B. N., Lapyonok, T., Holben, B. N., Sinyuk, A., Mishchenko, M. I. Yang, P., et al. (2002). Non-spherical aerosol retrieval method employing light scattering by spheroids. *Geophysical Research Letters*, *29*(10), 1415–1419.

Dubovik, O., Sinyuk, A., Lapyonok, T., Holben, B. N., Mishchenko, M. Yang, P., et al. (2006). Application of spheroid models to account for aerosol particle nonsphericity in remote sensing of desert dust. *Journal of Geophysical Research*, *111*(D11208), 1–34.

Feng, Q., Yang, P., Kattawar, G. W., Hsu, C. N., Tsay, S.-C., & Laszlo, I. (2009). Effects of particle nonsphericity and radiation polarization on retrieving dust properties from satellite observations. *Journal of Aerosol Science*, *40*(9), 776–789.

Forster, P., Ramaswamy, V., Artaxo, P., Berntsen, T., Betts, R., & Fahey, D. W. (Eds.). (2007). *Climate change 2007: the physical science basis. Contribution of Working Group I to the Fourth Assessment Report of the Intergovernmental Panel on Climate Change, Cambridge, United Kingdom*. New York, NY, USA: Cambridge University Press [Chapter 2].

Haywood, J., Francis, P., Osborne, S., Glew, M., Loeb, N. Highwood, E., et al. (2003). Radiative properties and direct radiative effect of Saharan dust measured by the C-130 aircraft during SHADE: 1. Solar spectrum. *Journal of Geophysical Research*, *108*(D18), 8577–8593.

Henning, Th., Il'in, V. B., Krivova, N. A., Michel, B., & Voshchinnikov, N. V. (1999). WWW database of optical constants for astronomy. *Astronomy & Astrophysics Supplement Series*, *136*, 405–406.

Hess, M., Koepke, P., & Schult, I. (1998). Optical properties of aerosols and clouds: The software package OPAC. *Bulletin of the American Meteorological Society*, *79*(5), 831–844.

Holben, B. N., Eck, T. F., Slutsker, I., Tanre, D., Buis, J. P. Setzer, A., et al. (1998). AERONET—A federated instrument network and data archive for aerosol characterization. *Remote Sensing of Environment*, *66*, 1–16.
Kahn, R., West, R., McDonald, D., Rheingans, B., & Mishchenko, M. (1997). Sensitivity of multi-angle remote sensing observations to aerosol sphericity. *Journal of Geophysical Research*, *102*(D14), 16861–16870.
Kalashnikova, O. V. Sokolik, I. N., et al. (2004). Modeling the radiative properties of nonspherical soil-derived mineral aerosols. *Journal of Quantitative Spectroscopy & Radiative Transfer*, *87*(2), 137–166.
Kaufman, Y. J., Tanré, D., & Boucher, O. (2002). A satellite view of aerosols in the climate system. *Nature*, *419*, 215–223.
King, M., Byrne, D., Herman, B., & Reagan, J. A. (1978). Aerosol size distributions obtained by inversions of spectral optical depth measurements. *Journal of the Atmospheric Sciences*, *35*(11), 2153–2167.
King, M. D., Kaufman, Y. J., Tanré, D., & Nakajima, T. (1999). Remote sensing of tropospheric aerosols from space: Past, present, and future. *Bulletin of the American Meteorological Society*, *80*(11), 2229–2259.
Kokhanovsky, A. (2003). Optical properties of irregularly shaped particles. *Journal of Physics D: Applied Physics*, *36*, 915–923.
Levoni, C., Cervino, M., Guzzi, R., & Torricella, F. (1997). Atmospheric aerosol optical properties: a database of radiative characteristics for different components and classes. *Applied Optics*, *36*(30), 8031–8041.
Levy, R., Remer, L., Mattoo, S., & Vermote, E. (2007). Second-generation operational algorithm: Retrieval of aerosol properties over land from inversion of moderate resolution imaging spectroradiometer spectral reflectance. *Journal of Geophysical Research*, *112*(D13211), 1–21.
Li, C., Kattawar, G. W., & Yang, P. (2004). Effects of surface roughness on light scattering by small particles. *Journal of Quantitative Spectroscopy & Radiative Transfer*, *89*, 123–131.
Liu, G. (2008). A database of microwave single-scattering properties for nonspherical ice particles. *Bulletin of the American Meteorological Society*, *89*(10), 1563–1570.
Mishchenko, M. I., & Travis, L. D. (1998). Capabilities and limitations of a current FORTRAN implementation of the T-matrix method for randomly oriented rotationally symmetric scatterers. *Journal of Quantitative Spectroscopy & Radiative Transfer 60*, *309-324*.
Mishchenko, M. I., Travis, L., & Lacis, A. (2003). Radiative transfer: Scattering. In J. R. Holton, J. Pyle, & J. A. Curry (Eds.), *Encyclopedia of atmospheric sciences*. San Diego: Academic Press.
Mishchenko, M. I., Travis, L. D., Rossow, W. B., & West, R. A. (1997). Modeling phase functions for dustlike tropospheric aerosols using a mixture of randomly oriented polydisperse spheroids. *Journal of Geophysical Research*, *102*(D12), 16831–16847.
Muñoz, O., & Volten, H. (2006). *Experimental light scattering matrices from the Amsterdam light scattering database. In Light scattering reviews*. Berlin: Springer.
Muñoz, O., Volten, H., Hovenier, J. W., Min, M., Shkuratov, Y. G. Jalava, J. P., et al. (2006). Experimental and computational study of light scattering by irregular particles with extreme refractive indices: Hematite and rutile. *Astronomy and Astrophysics*, *446*, 525–535.
Nakajima, T. (1996). Use of sky brightness measurements from ground for remote sensing of particulate polydispersions. *Applied Optics*, *35*, 2672–2686.
Nousiainen, T. (2009). Optical modeling of mineral dust particles: A review. *Journal of Quantitative Spectroscopy & Radiative Transfer*, *110*, 1261–1279.
Nousiainen, T., Kahnert, M., & Veihelmann, B. (2006). Light scattering modeling of small feldspar aerosol particles using polyhedral prisms and spheroids. *Journal of Quantitative Spectroscopy & Radiative Transfer*, *101*, 471–487.
Nousiainen, T., Muinonen, K., & Raisanen, P. (2003). Scattering of light by large Saharan dust particles in a modified ray optics approximation. *Journal of Geophysical Research*, *108*(D1), 4025–4042.
Nussenzveig, H. M. (1992). *Diffraction effects in semiclassical scattering*. London: Cambridge University.
Penttila, A., Zubko, E., Lumme, K., Muinonen, K., Yurkin, M. A. Draine, B., et al. (2007). Comparison between discrete dipole implementations and exact techniques. *Journal of Quantitative Spectroscopy & Radiative Transfer*, *106*, 417–436.
Purcell, E. M., & Pennypacker, C. R. (1973). Scattering and absorption of light by nonspherical dielectric grains. *Astrophysical Journal*, *186*, 705–714.
Ramanathan, V., Crutzen, P. J., Kiehl, J. T., & Rosenfeld, D. (2001). Aerosols, climate, and the hydrological cycle. *Science*, *294*(5549), 2119–2124.
Reid, E. A., Reid, J. S., Meier, M. M., Dunlap, M. R., Cliff, S. S. Broumas, A., et al. (2003). Characterization of African dust transported to Puerto Rico by individual particle and size segregated bulk analysis. *Journal of Geophysical Research*, *108*(D19).
Reid, J. S., Kinney, J. E., & Westphal, D. L. (2003). Analysis of measurements of Saharan dust by airborne and ground-based remote sensing methods during the Puerto Rico Dust Experiment (PRIDE). *Journal of Geophysical Research*, *108*(D19).
Schmidt, K., Wauer, J., Rother, T., & Trautmann, T. (2009). Scattering database for spheroidal particles. *Applied Optics*, *48*(11), 2154–2164.
Shell, K. M., & Somerville, R. C.J. (2007). Direct radiative effect of mineral dust and volcanic aerosols in a simple aerosol climate model. *Journal of Geophysical Research*, *112*(D03205), 1–15.
Sokolik, I. N., & Toon, O. B. (1998). Modeling the radiative properties of mineral aerosols for climate studies and remote sensing applications. *Journal of Aerosol Science*, *29*, S1199–S1200.
Sokolik, I. N., & Toon, O. B. (1999). Incorporation of mineralogical composition into models of the radiative properties of mineral aerosol from UV to IR wavelengths. *Journal of Geophysical Research*, *104*(D8), 9423–9444.
Sokolik, I., Winker, D., Bergametti, G., Gillette, D. A., Carmichael, G. Kaufman, Y. J., et al. (2001). Introduction to special section: outstanding problems in quantifying the radiative impacts of mineral dust. *Journal of Geophysical Research*, *106*(D16), 18015–18027.
Sun, W., Fu, Q., & Chen, Z. (1999). Finite-difference time-domain solution of light scattering by dielectric particles with perfectly matched layer absorbing boundary conditions. *Applied Optics*, *38*(15), 3141–3151.
Tegen, I., & Lacis, A. A. (1996). Modeling of particle size distribution and its influence on the radiative properties of mineral dust aerosol. *Journal of Geophysical Research*, *101*(D14), 19237–19244.
Twomey, S. (1977). *Introduction to the mathematics of inversion in remote sensing and indirect measurements*. New York: Elsevier.
Verhaege, C., Shcherbakov, V., & Personne, P. (2009). Retrieval of complex refractive index and size distribution of spherical particles from Dual-Polarization Polar Nephelometer data. *Journal of Quantitative Spectroscopy and Radiative Transfer*, *110*, 1690–1697.
Volten, H., Muñoz, O., Rol, E., de Haan, J. F., Vassen, W. Hovenier, J. W., et al. (2001). Scattering matrices of mineral aerosol particles at 441.6 nm and 632.8 nm. *Journal of Geophysical Research*, *106*(D15), 17375–17401.
Volten, H., Muñoz, O., Brucato, J. R., Hovenier, J. W., Colangeli, L. Waters, L. B.F. M., et al. (2006). Scattering matrices and reflectance spectra of forsterite particles with different size distributions. *Journal of Quantitative Spectroscopy and Radiative Transfer*, *100*, 429–436.
Waterman, P. C. (1965). Matrix formulation of Electromagnetic scattering. *Proceedings of the IEEE*, *53*, 805–812.
West, R. A., Doose, L. R., Eibl, A. M., Tomasko, G., & Mishchenko, M. (1997). Laboratory measurements of mineral dust scattering phase function and linear polarization. *Journal of Geophysical Research*, *102*(D14), 16871–16881.
Yang, P., Feng, Q., Hong, G., Kattawar, G. W., Wiscombe, W. J. Mishchenko, M., et al. (2007). Modeling of the scattering and radiative properties of nonspherical dust-like aerosols. *Journal of Aerosol Science*, *38*(10), 995–1014.
Yang, P., & Liou, K. N. (1996a). Finite-difference time domain method for light scattering by small ice crystals in three-dimensional space. *Journal of Optical Society of America A*, *13*(10), 2072–2085.
Yang, P., & Liou, K. N. (1996b). Geometric-optics-integral-equation method for light scattering by nonspherical ice crystals. *Applied Optics*, *35*(33), 6568–6584.
Yang, P., Liou, K. N., Mishchenko, M. I., & Gao, B. C. (2000). Efficient finite-difference time domain scheme for light scattering by dielectric particles: application to aerosols. *Applied Optics*, *39*(21), 3727–3737.
Yang, P., Kattawar, G. W., & Wiscombe, W. J. (2004). Effect of particle asphericity on single-scattering parameters: comparison between Platonic solids and spheres. *Applied Optics*, *43*(22), 4427–4435.

Yee, K. (1966). Numerical solution of initial boundary value problems involving Maxwell's equations in isotropic media. *Antennas and Propagation, IEEE Transactions on Antennas and Propagation*, *AP-14*(8), 302–307.

Yurkin, M.A., Hoekstra, A.G., (2009). *User Manual for the Discrete Dipole Approximation Code* ADDA v. 0.79, http://a-dda.googlecode.com/svn/tags/rel_0_79/doc/manual.pdf.

Zubko, E., Muinonen, K., Shkuratov, Y., Videen, G., & Nousiainen, T. (2007). Scattering of light by roughened Gaussian random particles. *Journal of Quantitative Spectroscopy & Radiative Transfer*, *106*(1-3), 604–615.